Quirks at the Tevatron and beyond

Roni Harnik, Graham D. Kribs, and Adam Martin

Phys. Rev. D **84**, 035029 — Published 26 August 2011

DOI: 10.1103/PhysRevD.84.035029

FERMILAB-PUB-11-271-T

Quirks at the Tevatron and Beyond

Roni Harnik,[1] Graham D. Kribs,[1,2] and Adam Martin[1]

[1] *Theoretical Physics Department, Fermilab, Batavia, IL 60510*
[2] *Department of Physics, University of Oregon, Eugene, OR 97403*

We consider the physics and collider phenomenology of quirks that transform nontrivially under QCD color, $SU(2)_W$ as well as an $SU(N)_{ic}$ infracolor group. Our main motivation is to show that the recent Wjj excess observed by CDF naturally arises in quirky models. The basic pattern is that several different quirky states can be produced, some of which β-decay during or after spin-down, leaving the lightest electrically neutral quirks to hadronize into a meson that subsequently decays into gluon jets. We analyze LEP II, Tevatron, UA2, and electroweak precision constraints, identifying the simplest viable models: scalar quirks ("squirks") transforming as color triplets, $SU(2)_W$ triplets and singlets, all with vanishing hypercharge. We calculate production cross sections, weak decay, spin-down, meson decay rates, and estimate efficiencies. The novel features of our quirky model includes: quirkonium decay proceeds into a pair of gluon jets, without a b-jet component; there is essentially no associated Zjj or γjj signal; and there are potentially new (parameter-dependent) contributions to dijet production, multi-W production plus jets, $W\gamma$, $\gamma\gamma$ resonance signals, and monojet signals. There may be either underlying event from low energy QCD deposition resulting from quirky spin-down, and/or qualitatively modified event kinematics from infraglueball emission.

I. INTRODUCTION

CDF has recently reported a 4.1σ excess in the Wjj event sample in 7.3 fb^{-1} of data for dijet invariant masses between $120 - 160$ GeV [1, 2]. The excess comprises of hundreds of events in the $\ell jj + \not{E}_T$ channel, corresponding to a sizeable cross section, $\sigma \sim$ few pb to account for the smaller leptonic branching fraction and the efficiency of detecting the signal. Several explanations have already appeared [3, 4], as well as detailed discussion of the size and shape of the Standard Model (SM) background [5].

In this paper we present an explanation of this excess invoking pair production of "quirks" [7], defined below, which subsequently undergo radiative energy loss and weak decay, finally annihilating into dijets. There are two main pathways that begin with quirk production and end with a Wjj signal consistent with the CDF analysis after their cuts: The first path consists of electroweak production of a heavy-light quirk pair, where the heavy quirk β-decays into a light quirk, emitting a $W^\pm$, and then the remaining quirk–anti-quirk system settles into a quirkonium ground state. The quirkonium decays into gluon jets that reconstruct an invariant mass peak. The second path consists of strong production of a heavy quirk-anti-quirk pair, where both quirks β-decay to their lighter electroweak partners. Even though two W bosons are emitted in this process, one W decay can be missed by the CDF analysis, particularly when the decay products are light quark jets that have energies below the CDF jet energy cuts. Schematic diagrams of the production and decay of the heavy-light quirk system and the heavy-heavy quirk system is shown in Fig. 1.

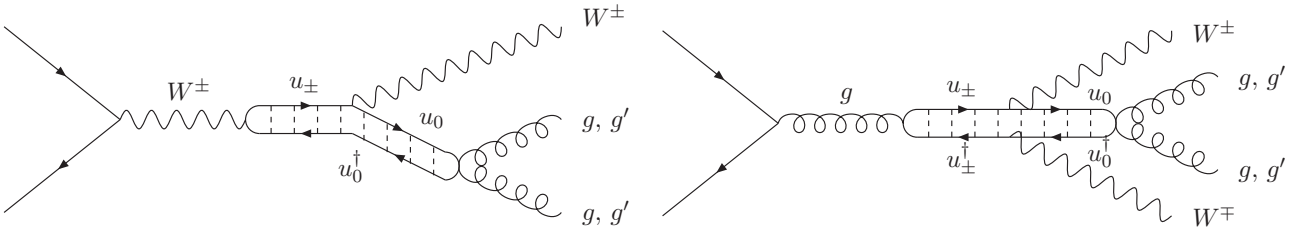

FIG. 1. Two classes of squirk pair production and β-decay that can lead to a Wjj final state with a dijet invariant mass peak are shown in schematic diagrams. The top, "one-armed lobster" diagram corresponds to weak production $p\bar{p} \to W^* \to u_\pm u_0^\dagger + u_0 u_\mp^\dagger$, following by charged squirk β-decay $u_\pm \to W^\pm u_0$, and finally annihilation of the neutral quirks into a pair of gluons or infragluons (g'). The bottom, "two-armed lobster" diagram corresponds to strong production of a heavy quirk-anti-quirk pair, following by β-decay of both heavy squirks, and finally annihilation of the neutral quirks into gluons. The latter production can pass the CDF analysis with a modest efficiency when the decay products of one of the W's are not detected. Quirky spin-down radiation (into color gluons, infracolor glueballs, etc.) is not shown for either diagram.

In this paper we consider "squirks" – the scalar analogues of "quirks" [6, 7], which are new fields transforming under part of the SM gauge group along with a new strongly-coupled "infracolor" group $SU(N)_{ic}$. The strong coupling scale of the infracolor group, Λ_{ic}, is assumed to be much smaller than the masses of all quirky (or squirky) fields transforming under infracolor. Consequently, infracolor strings do not break, and quirk (or squirk) pairs remain in a bound state even when they are produced with high kinetic energies. This leads to several interesting collider physics, model building and dark matter applications [7–21]. (Other work on hidden valley models can be found in [22–24].) Certain kinds of quirks have already been searched for at the Tevatron by the D0 collaboration [26]. Typically, squirks and quirks transform as a vector-like representation of the SM gauge group as well as a vector-like representation of infracolor, and thus can acquire any mass without any additional Higgs sector.[1]

Here is a summary of our basic strategy to explain the Wjj signal, while avoiding the many constraints from LEP II, Tevatron, and UA2:

1. We consider squirks (scalars), rather than quirks (fermions), mainly to employ a renormalizable operator to lead to mass splittings, while also minimizing the electroweak precision contribution resulting from this splitting.

2. The Wjj signal arises from a combination of the two distinct squirk pair production processes shown in Fig. 1. The weak decay, $u_\pm \to W^\pm u_0$, could be 2-body or 3-body, depending on the mass splitting between $u_\pm$ and u_0.

3. All of the squirks are color triplets under QCD. Hence, the leading visible annihilation channel of a squirk–anti-squirk bound state system is into gg. This provides our source of the jet-jet resonance, and consequently, we predict the flavor of the jets in the excess observed by CDF to be pure glue with no heavy flavor.

[1] Noteable exceptions, where quirks acquire masses through electroweak symmetry breaking, can be found in Refs. [16, 20].

	$SU(N)_{ic}$	$SU(3)_c$	$SU(2)_L$	$U(1)_Y$
U	**N**	**3**	**3**	0
S	**N**	**3**	**1**	0

TABLE I. Scalar quirk quantum numbers.

4. The electrically-neutral squirks are mixtures among the $T_3 = 0$ component of an electroweak triplet as well as an electroweak singlet. Hence, they do not couple to the γ or the Z. This implies the tree-level production cross section of the lightest squirks at LEP II vanishes.

5. The electrically-charged squirks have masses larger than 100 GeV, and so are beyond the LEP II sensitivity.

6. Light squirk pair production $u_0 u_0^\dagger$ results in a dijet invariant mass around $150 - 160$ GeV. The production cross section is far smaller than Tevatron's dijet sensitivity [27], making it safe from Tevatron searches. The production cross section of this resonance at the CERN SppS ($\sqrt{s} = 630$ GeV) collider is less than 1 pb per infracolor. The UA2 bound is roughly 90 pb [28], and thus does not restrict N_{ic}.

At this point we should emphasize that some aspects of squirk production and decay can be calculated or simulated with standard collider tools, but some cannot and one must resort to estimates or parameterization of the various possibilities. What *can* be calculated unambiguously is i) squirk pair production (at leading order, far from the cross section threshold), ii) the weak decay rate of squirks (from which we use to infer the weak decay of the squirky mesons), and iii) squirky meson annihilation rates into Standard Model fields. What *cannot* be calculated reliably is the dynamics of the "spin-down" process, as the high energy squirks shed their momentum to settle into a (near) ground state squirky meson, and the spectrum and content of the resulting radiation. An attempt at modeling this radiation is underway [21]. As a consequence, we do not attempt a full simulation of squirky production. Instead, we calculate quantities that are under control, with estimates of signal efficiencies, and point out where simulations could improve our understanding. To deal with the remaining uncertainties due to non-perturbative infracolor dynamics we discuss some of the possible scenarios for this spin down and their effects on phenomenology in Sec. IV.

II. MODEL

We extend the Standard Model to include one set of squirks, U and S with quantum numbers given in Table I. The gauge-invariant operators involving these fields include the mass terms

$$\frac{1}{2}M_U^2 U^\dagger U + \frac{1}{2}M_S^2 S^\dagger S \tag{1}$$

and quartic interactions including

$$\begin{aligned}&\lambda_4(S^\dagger S)(U^\dagger U) + \lambda_U(H^\dagger H)(U^\dagger U) + \lambda_S(H^\dagger H)(S^\dagger S)\\ &+ \lambda_{U4}(U^\dagger U)^2 + \lambda_{S4}(S^\dagger S)^2\end{aligned} \tag{2}$$

as well as

$$\kappa(H^\dagger \tau^a H)(S^\dagger U_a) + \text{h.c.}\,. \tag{3}$$

The operators proportional to $\lambda_{U,S}$ lead to shifts in the masses of U and S, as well as Higgs boson trilinear and quartic interactions with $U^\dagger U$, $S^\dagger S$. The operators proportional to $\lambda_{U4,S4}$ will turn out to affect certain annihilation channels. Since our analysis does not depend on the existence of these interactions, we do not consider them further.

The triplet field U can be written in terms of its isospin components

$$U = \begin{pmatrix} U_1 \\ U_2 \\ U_3 \end{pmatrix} \tag{4}$$

where we can rewrite the fields in the mass eigenstate basis with definite electric charges,

$$u_\pm \equiv \frac{1}{\sqrt{2}}\left(U_1 \mp i U_2\right) \tag{5}$$

This is completely analogous to the rewriting of the usual triplet of $SU(2)_L$ of gauge bosons $W_{1,2,3}$ into $W^{\pm,0}$.

After electroweak symmetry breaking, the Higgs doublet can be written as $H = (v+h)\exp[i\Pi]/\sqrt{2}$ in terms of the vacuum expectation value $v \equiv 246$ GeV, the physical Higgs boson h, and the nonlinear representation of the Goldstone bosons, contained within Π. Expanding the operator Eq. (3) to second order in Π, one can verify that only $(v+h)$ enters the dynamics, and thus we can ignore the Goldstone interactions.

The central implication of Eq. (3) is that it causes the singlet $S^\dagger$ to mix with the neutral component of the triplet U_3, enlarging the mass splitting between them. The two mass eigenstates, which we call u_0 and u_1 for the light and heavy states, have masses of

$$m_0^2 = \frac{1}{2}\left(m_U^2 + m_S^2 - \sqrt{(m_U^2 - m_S^2)^2 + 4\delta^4}\right) \tag{6}$$

$$m_1^2 = \frac{1}{2}\left(m_U^2 + m_S^2 + \sqrt{(m_U^2 - m_S^2)^2 + 4\delta^4}\right) \tag{7}$$

where $\delta \equiv \sqrt{\kappa v^2/2}$. These neutral squirks are mixtures of the singlet and triplet

$$\begin{pmatrix} u_0 \\ u_1 \end{pmatrix} = \begin{pmatrix} c_\theta & -s_\theta \\ s_\theta & c_\theta \end{pmatrix} \begin{pmatrix} S \\ U_3 \end{pmatrix} , \tag{8}$$

where we have used the notation $c_\theta \equiv \cos\theta$, $s_\theta \equiv \sin\theta$, and the neutral state mixing angle is

$$\tan 2\theta = \frac{2\delta^2}{m_U^2 - m_S^2} . \tag{9}$$

The charged squirk masses remain unchanged with mass $m_\pm = M_U$.

Due to infracolor confinement, the squirks remain in a bound state. The dynamics of the squirk bound states will occupy much of the later discussion of the paper. We work in the approximation that $\alpha_{ic}(m_q) \ll 1$, so that the masses of the bound states are dominated by the constituent squirk masses. There is a hierarchy of mesons formed from orbital excitations of the bound squirks. We will be concerned mainly with just the $J = L = 0$ (with necessarily $S = 0$ for squirks) ground states, which we write as η_{ij} with ij labeling the constituent squirks. The charged bound states consist of

$$\eta_{\pm 0} \sim (u_\pm u_0^\dagger), (u_0 u_\mp^\dagger) \tag{10}$$

$$\eta_{\pm 1} \sim (u_\pm u_1^\dagger), (u_1 u_\mp^\dagger) , \tag{11}$$

where the charged meson masses are roughly $m_{\eta_{\pm i}} \simeq m_\pm + m_i$. The neutral states consist of several distinct mass eigenstates

$$\eta_{00} \sim (u_0 u_0^\dagger) \tag{12}$$

$$\eta_{+-} \sim (u_+ u_+^\dagger), (u_- u_-^\dagger) . \tag{13}$$

$$\eta_{11} \sim (u_1 u_1^\dagger) \tag{14}$$

with masses that are again roughly $m_{\eta_{00}} \simeq 2m_0$, $m_{\eta_{+-}} \simeq 2m_\pm$, and $m_{\eta_{11}} \simeq 2m_1$. Whether the heavier squirks hadronize before weak decay, like the b-quark of the SM, or decay before hadronization, like the t-quark of the SM, depends on the parameters of the model. As we will see, both regimes are relevant to the model.

III. SQUIRK PRODUCTION

Squirks can be produced through color and electroweak production. Conservation of infracolor implies squirks are always produced in pairs. At hadron colliders, squirks are generically produced with some kinetic energy for each squirk. As vividly demonstrated in [7], squirks will initially fly apart forming an infracolor string between them. The string will stretch without tearing until the energy in the infracolor string matches the total kinetic energy. The infracolor scale of interest to us is roughly $\Lambda_{\rm QCD} \lesssim \Lambda_{ic} \ll m_{\rm squirk}$, where the infracolor strings are *microscopic*, and thus the squirks shed their kinetic energy and annihilate on timescales short compared with the timing systems of the collider detectors.

Here we consider the several possible combinations of squirk pair production in terms of the squirk mass eigenstates.

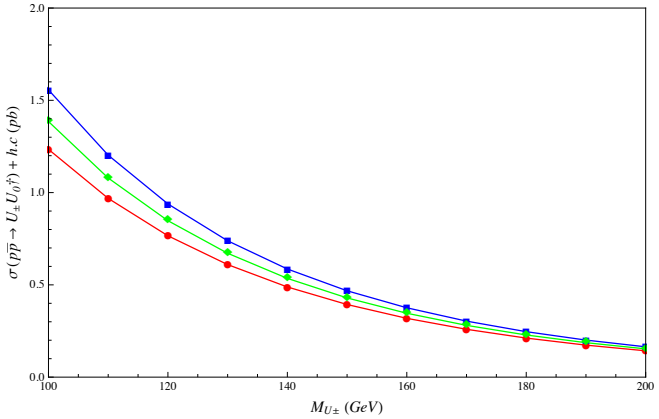

FIG. 2. Leading order production cross section at Tevatron $\sigma(u_\pm u_0^\dagger + u_0 u_\mp^\dagger)$. The three contours correspond to three choices of $m_0 = 75, 80, 85$ GeV from top to bottom. The cross section shown in this figure includes the QCD color factor and both electric charges, but *does not* include the infracolor (enhancement) factor, nor the mixing angle (suppression) associated with the U_3 component of u_0.

A. $u_\pm u_0^\dagger + u_0 u_\mp^\dagger$

The production of charged plus neutral squirks proceeds through a s-channel $W^\pm$. This cross section is enhanced by the number of QCD colors and infracolors, while suppressed by the mixing angle associated with the U_3 component of u_0. The cross section at the Tevatron is shown in Fig. 2, incorporating the QCD color factor enhancement, but without the infracolor enhancement as well as without the neutral state mixing angle suppression, to remain as general as possible at this point.

Once squirks are produced, numerous effects must be considered to obtain a realistic estimate of the signal rates. This includes understanding the spin-down process, β-decay, and the various annihilation channels. In addition, signal efficiencies are non-trivial when $m_\pm - m_0 \lesssim M_W$ and thus the W decay is off-shell. This case, which is relevant for our model, implies the lepton p_T cuts tend to slice away more signal while also changing the dijet kinematics. A full estimation of our signal efficiency is not possible given the unknowns regarding the quirky spin-down dynamics. Instead, we have performed estimates of signal efficiency by constructing a "stand in" model, similar to Ref. [3]. This is discussed in Sec. VII.

B. $u_0 u_0^\dagger$ and $u_1 u_1^\dagger$

The electroweak quantum numbers of u_0 and u_1 ($T_3 = 0$, $Q = 0$) imply the couplings to γ and Z exactly vanish, which has important implications. The first, and perhaps most important, is that u_0 and u_1 cannot be pair-produced at LEP II at tree-level.[2] Second, the bound states formed from $u_0 u_0^\dagger$ and $u_1 u_1^\dagger$ cannot decay into pairs of photons or (potentially off-shell) Zs.

The neutral squirks, u_0 and u_1, can be pair-produced through QCD. The Tevatron production cross section of neutral squirk pairs is shown in Fig. 3. The lightest bound state of squirks must ultimately annihilate back into SM particles. There are several final state topologies that can result: gg and $g'g'$ (infragluon pair), illustrated in Fig. 4, as well as W^+W^- (not shown).

Although our model has negligible LEP II production of squirks, it is amusing to consider the size of the cross section for generalized squirks with (Q, T_3) arbitrary. We find that cross section for colored squirks is roughly 0.6 pb for $Q = 0, |T_3| = 1/2$. The cross section increases if $Q \neq 0$ is taken. Since the total hadronic cross section at LEP II is measured to within ± 0.5 pb to 95% CL [29], even without considering the distinctive kinematics (dijet invariant mass peak), we see that 80 GeV squirks transforming under the electroweak group are essentially ruled out. This is the motivation for our model employing an electroweak triplet that carries vanishing hypercharge.

[2] There is a set of one-loop diagrams involving virtual Ws and virtual $u_\pm$ exchange, but this is very small.

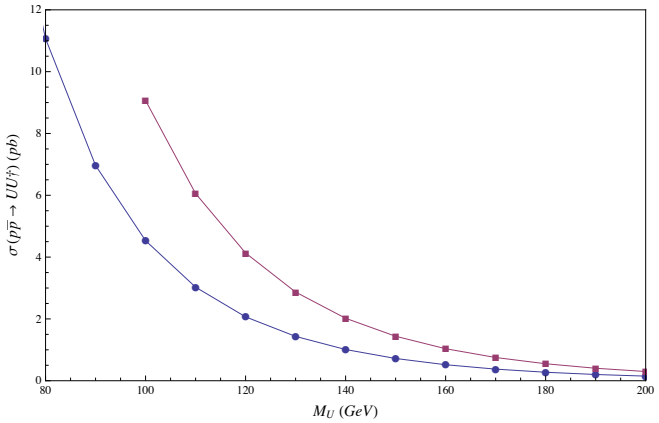

FIG. 3. Leading order production cross sections at Tevatron for $\sigma(u_\pm u_\pm^\dagger)$ with (top curve; $M_U \to m_\pm$) and $\sigma(u_0 u_0^\dagger)$ or $\sigma(u_1 u_1^\dagger)$ (bottom curve; $M_U \to m_0$ or m_1). Again, like Fig. 2, the cross sections include the QCD color factor and both electric charges, but do not include the infracolor factor.

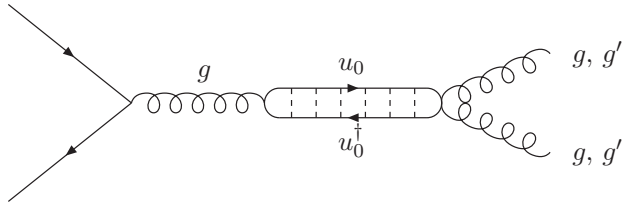

FIG. 4. One of several diagrams illustrating squirky pair production through QCD of the lightest electrically-neutral squirks $p\bar{p} \to u_0 u_0^\dagger$ and annihilation $u_0 u_0^\dagger \to gg$. Radiation (into color gluons, infracolor glueballs, etc.) is not shown.

C. $u_\pm u_\pm^\dagger$

Charged squirk pair production, possible β-decay, spin-down, and annihilation is a fascinating but intricate process. Charged squirk pairs can be produced through QCD, and so their production rate at hadron colliders is large. The cross section at the Tevatron is shown in Fig. 3.

The signature of charged squirks depends crucially on the various competing timescales of spin-down, β-decay, and annihilation. If both charged squirks were to rapidly β-decay, $u_\pm \to W^\pm u_0$, this leads to a $W^+W^- u_0 u_0^\dagger$ signal, with $u_0 u_0^\dagger$ annihilating into gg (or invisibly to $g'g'$). Whether this process is a *feature* or a *constraint* depends on several factors, particularly, the mass splitting $m_\pm - m_0$ and the associated efficiency of detecting the W decay products.

There is, however, another process that competes with β-decay, namely the squirky spin-down and annihilation. As we will show in the next few sections, there is a region of parameter space where the spin-down and annihilation of $u_\pm u_\pm^\dagger$ occurs *faster* than β-decay, leading to gg, $g'g'$, $\gamma\gamma$, and W^+W^- signatures.

D. $u_\pm u_1^\dagger + u_1 u_\mp^\dagger$

The production of the charged plus the *heavier* neutral squirk proceeds through a s-channel $W^\pm$ just like Sec. III A. This cross section is enhanced by the number of QCD colors and infracolors, while suppressed by the mixing angle of the U_3 component of u_1. While this process has a substantially smaller cross section than the one with u_0, there are several interesting signatures. First, if the β-decay process $u_1 \to W^\pm u_\mp$ occurs quickly, then this process contains the same rich phenomenology of Sec. III C along with an additional $W^\pm$, which itself could be off-shell. If instead spin-down occurs rapidly, then a competition is set up between β-decay with subsequent annihilation of η_{+-}, versus direct annihilation $\eta_{+1} \to W\gamma$. It is also possible that β-decay of $u_\pm \to W^\pm u_0$ occurs, forcing $u_1 \to W^\pm u_\mp$ followed by $u_\mp \to W^\mp u_0$. This gives a spectacular three-W plus 2-jet signal.

As we will see in the next several sections, the production of $u_0 u_0^\dagger$, $u_1 u_1^\dagger$, and $u_\pm u_\pm^\dagger$ are most relevant for the Wjj signal.

IV. WEAK DECAY AND SPIN-DOWN

We now consider the quirky dynamics that occurs after the squirk pair is produced. This includes β-decay, spin-down, and the annihilation of the squirks into SM fields. The annihilation cross section itself is a sensitive decreasing function of the angular momentum of the squirk system. The angular momentum of the system is of order $L \sim 1$ in the hard production, and then grows as the excited state losses energy through radiation. Since every radiated quantum is expected to change the angular momentum by $\Delta L \sim \pm 1$, L grows roughly as the square root of the number of emitted quanta. As a result, the squirky bound state typically loses its excitation energy *before* annihilation [7]. On the other hand, β-decay can occur during the energy loss process, as it is independent of angular momentum. Thus, in this section we discuss the competition between β-decay and energy loss, and then in Sec. V we calculate the decay rates of squirkonium states formed only after energy loss has occurred.

A. β-decay

Weak decay of bound squirks or quirks can be readily approximated by considering the decay of an individual squirk in isolation. This is entirely analogous to heavy quark decay of (heavy) quarkonia in the SM. Charged and heavy neutral squirks can β-decay through $u_\pm \to W^{\pm} u_0$ and $u_1 \to W^{\pm} u_\mp$. When the mass splitting among these states $\Delta m_i = |m_\pm - m_i|$ is smaller than M_W, which is the main parameter region of interest to us, the rate is given by

$$\Gamma_\beta(u_\pm \to W^{\pm *} u_0) = \frac{N_f G_F^2 s_\theta^2 R(m_\pm, m_0, m_W)}{48\pi^3} \tag{15}$$

where the function R is presented in its full glory in Appendix B. The kinematic function R scales approximately as $|\Delta m|^5$, as expected for a 3-body decay. The mixing angle is defined by the transformation given in Eq.(8). The rate scales as the number of SM flavors and colors to decay into, N_f, which is 9 for $m_\tau < |\Delta m| < m_t + m_b$. The rate for $u_1 \to W^{\pm} u_\mp$ is analogous,

$$\Gamma_\beta(u_1 \to W^{\mp *} u_\pm) = \frac{N_f G_F^2 s_\theta^2 R(m_1, m_\pm, m_W)}{24\pi^3} \ , \tag{16}$$

where the relative factor of 2 (compared with the charged squirk case) accounts for the two possible electric charge combinations. The inverse decay rate is roughly

$$t_{\beta, u_\pm} \sim (3 \times 10^{-21} \text{ sec}) \times \left(\frac{40 \text{ GeV}}{\Delta m_0}\right)^5 \left(\frac{0.717}{s_\theta}\right)^2 \ . \tag{17}$$

B. Spin-down

The "spin-down" or energy loss process for squirks transforming under both QCD and infracolor is an interesting but difficult problem. In general, the energy loss can proceed through the radiation of a) regular QCD hadrons – mostly charged and neutral pions, or b) infracolor glueballs.[3] Given the intrinsically non-perturbative nature of this emission, we will not assert which of these two distinct processes dominates, but instead simply make estimates assuming one or the other does, and discuss the phenomenology.

One reasonable approach to the mechanism of energy loss is to assume that at every squirky oscillation, the two QCD-hadronized squirks at the end of the infracolor string collide at semi-relativistic velocities, emitting a soft hadron, carrying energy roughly of order $\Lambda_{\rm QCD}$ or Λ_{ic} [7, 21]. The period of the squirk oscillations is of order μ/Λ_{ic}^2, where μ is the reduced mass of the two-squirk system.

Consider first the case where only QCD dominates and the excited squirky system loses energy of order $\Delta E \sim \Lambda_{\rm QCD} \sim 1$ GeV after every oscillation.[4] The time to lose the total excitation energy $E_{ij} = \sqrt{\hat{s}} - (m_i + m_j)$ for

[3] Photons may also play an important role [11] in the case where quirks or squirks are charged and uncolored, but this will be subdominant to QCD radiation for our model.

[4] It is not unreasonable for the energy loss process to be dominated by QCD due to kinematics. This is because QCD contains pions, which are lighter than glueballs, unlike the situation with infracolor.

$(i, j = 0, 1, \pm)$ is roughly

$$t_{\rm loss}(E_{ij}) \sim \frac{\mu}{\Lambda_{ic}^2}\frac{E_{ij}}{\Lambda_{\rm QCD}} \tag{18}$$
$$\sim \left(\frac{\mu}{50\ {\rm GeV}}\right)\left(\frac{1\ {\rm GeV}}{\Lambda_{ic}}\right)^2\left(\frac{E_{ij}}{100\ {\rm GeV}}\right)\left(\frac{1\ {\rm GeV}}{\Lambda_{\rm QCD}}\right)$$
$$\times\ (3\times 10^{-21}\ {\rm sec})\ .$$

For the case $(i, j) = (\pm, 0)$, the reduced mass $\mu = 48 \to 53$ GeV for $m_\pm \to 120 \to 160$ GeV. Thus, we see that a typical excited squirkonium system settles down to its ground state on a timescale roughly comparable to β-decay, Eq. (17), when $|\Delta m| \simeq 40$ GeV. We stress that this mass difference is a rough approximation, given that we cannot determine the energy loss rate precisely. In this scenario, every squirky event will be accompanied by a large multiplicity of soft pions which will contribute to the underlying event. Such new contributions to underlying event physics were studied in [11, 21].

Next, consider the case where the energy is lost also through infracolor glueball emission. This emission proceeds in addition to the QCD emission described above, and so the timescale in Eq. (18) is expected to be an upper bound. Infracolor glueballs generically have long lifetimes [7], and thus will escape the detector as missing energy. If infracolor glueball emission does dominate the spin-down process, then there is additional missing energy in every squirky event. This affects the p_T distribution and particularly the $\not{E}_T$ distributions of squirk signals, but we will not study this effect here (for a different study on the effects of hidden radiation see [18]).

C. Survival Probability

We can be more precise about our estimate for the fraction of squirk production that β-decays before settling into the ground state η. This calculation involves convoluting the differential distribution $d\sigma_{ij}/dE_{ij}$ with the survival probability, $P(E_{ij}) = 1 - \exp[-t_{\rm loss}(E_{ij})/t_{ij}]$ to obtain branching fractions:

$${\rm BR}(u_\pm u_0^\dagger \to \eta_{\pm 0}) = \frac{1}{\sigma_{\pm 0}}\int dE_{\pm 0}\frac{d\sigma_{\pm 0}}{dE_{\pm 0}}P(E_{\pm 0}) \tag{19}$$

$${\rm BR}(u_\pm u_0^\dagger \to W^\pm u_0 u_0^\dagger) = 1 - {\rm BR}(u_\pm u_0^\dagger \to \eta_{\pm 0})\ , \tag{20}$$

where $t_{\pm 0} = t_{\beta, u_\pm}$, and

$${\rm BR}(u_+ {u_+}^\dagger \to \eta_{+-}) = \frac{1}{\sigma_{+-}}\int dE_{+-}\frac{d\sigma_{+-}}{dE_{+-}}P(E_{+-}) \tag{21}$$

$${\rm BR}(u_+ {u_+}^\dagger \to W^+W^- u_0 u_0^\dagger) = 1 - {\rm BR}(u_+ {u_+}^\dagger \to \eta_{+-})\ . \tag{22}$$

where $t_{+-} = t_{\beta, u_\pm}/2$, where the factor of $1/2$ accounts for β-decay of either squirk. Lastly, for completeness, we emphasize that the lightest squirks cannot β-decay, and thus lose energy to the ground state with unity probability, i.e.,

$${\rm BR}(u_0 u_0^\dagger \to \eta_{00}) = 1\ . \tag{23}$$

Here this branching ratio assumes the squirks lose energy before they annihilate, which is our working assumption for this paper [7, 11]. We use these results for our signal estimates in Sec. VI.

V. ANNIHILATION

Squirk pairs will eventually settle into a ground state, η, which itself decays through constituent squirk annihilation analogous to quark annihilation leading to meson decay in QCD.

In this section we compute the decay rates of the various squirkonium states into SM fields and infragluons. The formalism for calculating the annihilation rates is similar to that of calculating the decay rate of quarkonium in QCD [30] which has been adapted to quirkonium in [7, 9, 10, 20]. Moreover, squirkonium has a close relative in

supersymmetry, "stoponium", whose decay rates have computed [31–33], and we use to cross-check our own results. Under the assumption that the squirks settle into the ground state, η ($J^{PC} = 0^{-+}$), the decay of $\eta \to \bar{f}f$ is negligible, and will not be considered for the remainder of the paper.

The squirkonium decay rate is

$$\Gamma \sim \sigma v_{\rm rel} \left|\psi(0)\right|^2 \tag{24}$$

where σ is the annihilation cross section in question, $v_{\rm rel}$ is the relative velocity among the quirks and $\left|\psi(0)\right|^2$ is the squared wave function of the squirkonium bound state evaluated at zero squirk separation. The annihilation flux $\sigma v_{\rm rel}$ is evaluated near threshold, where the two squirks are nearly at rest. Assuming the squirk wave function is Coulombic, the squared wave function is

$$\left|\psi(0)\right|^2 = c_\eta \frac{a_0^{-3}}{\pi} \tag{25}$$

where a_0 is the Bohr radius given by

$$a_0 = \left[\left(C_2(\mathbf{3})\alpha_s(a_0^{-1}) + C_2(\mathbf{N}_{ic})\alpha_{ic}(a_0^{-1})\right)\mu\right]^{-1}. \tag{26}$$

Note that there may be significant deviations from the Coulombic result as well as other QCD and infracolor effects. This can be partly parameterized by a coefficient, c_η, as discussed in Ref. [16]. In practice, higher order QCD and infracolor effects can significantly modify the Coulombic estimate, as can be found by scaling the QCD results of [34] to include infracolor as well as color. An additional assumption in our calculations is that we assume the N_{ic} dependence of the wavefunction associated with the initial bound state of a pair of squirks is to be treated the same way as the N_c dependence of QCD for quarkonia. In any case, we do not attempt to model the squirkonium potential beyond the Coulombic approximation, and thus take $c_\eta = 1$ for our estimates of the absolute widths of η.

Now we consider the several possible annihilation channels for the squirky mesons according to the constituent squirk states.[5]

A. η_{00}, η_{11}

All of the neutral mesons can decay into QCD gluons and infracolor gluons, with decay rates

$$\Gamma(\eta_{ii} \to gg) = \frac{4\pi N_{ic}\alpha_s^2}{3m_i^2}\left|\psi(0)\right|^2 \tag{27}$$

$$\Gamma(\eta_{ii} \to g'g') = \frac{3\pi(N_{ic}^2-1)\alpha_{ic}^2}{2N_{ic}m_i^2}\left|\psi(0)\right|^2, \tag{28}$$

for $i = 0, 1$. These rates are parton-level approximations without QCD or infracolor hadronization. In the limit $\Lambda_{\rm QCD}, \Lambda_{ic} \ll m_0$, the effects of hadronization on the decay widths is small [35]. Since u_i does not carry electric charge, the tree-level width of $\eta_{ii} \to \gamma\gamma$ vanishes. There is also potentially a tree-level rate into W^+W^- through a t/u-channel $u_\pm$. This rate is suppressed by kinematics (particularly for $\eta_{00} \to W^+W^-$, since $m_0 \simeq M_W$) as well as the weak couplings associated with this channel. While potentially interesting for η_{11}, which can be copiously produced at LHC, it is subleading compared with the above glue and infraglue rates, and we do not consider it further.

The gg channel can dominate, allowing $u_0 u_0^\dagger$ production at a hadron collider to lead to a dijet bump. For the Tevatron, the production rate is far smaller than the QCD background, leading to neither an observable signal nor a constraint [27]. Interestingly, UA2 has comparatively strong bounds on dijet resonances. The production cross section $\sigma(u_0 u_0^\dagger)$ at UA2 ($\sqrt{s} = 630\,\text{GeV}$) with $m_0 = 80$ GeV is less than 1 pb per infracolor. Assuming $u_0 u_0^\dagger$ quickly spins down and annihilates into a dijet resonance of about 160 GeV, the limit we should compare to is the W'/Z' limit at the same mass. This is $\sigma(\text{dijet}) < 90$ pb for $M_{W'/Z'} = 160$ GeV, and so is completely safe.

The next comparable channel is annihilation into infragluons: $g'g'$. The signature of the $g'g'$ topology depends on the decay rate of the infragluballs formed from the infragluon emission. The infragluball decay rate is generally extremely small, since it proceeds through a dimension-8 operator suppressed by squirk masses [7]. Infragluballs are thus expected to escape the detector before they decay. In this case, the $g'g'$ signal is itself invisible. There can also be a $gg'g'$ process, when the squirks are produced in association with an additional initial- or final-state gluon (or quark) jet, leading to a monojet signal.

[5] There is also the possibility that quirks or squirks could form "hybrid mesons" in which the quirk pair is in an infracolor non-singlet state [25], leading to a set of qualitatively different decay processes. These include the single emission of glue or infraglue, combined with another SM gauge boson. The dynamics of infracolor non-singlets is very difficult to estimate without a more complete picture of the quirky hadronization dynamics, and so we do not consider it further.

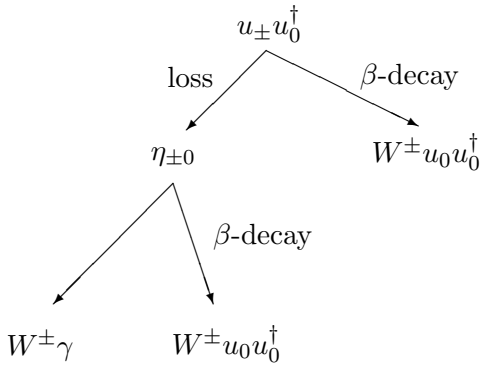

FIG. 5. The "tree of life" for the charged + neutral squirk pair. While only $u_\pm u_0^\dagger$ is shown, the same tree of life also applies to $u_0 u_\pm^\dagger$.

B. $\eta_{\pm 0}$

The $\eta_{\pm 0}$ represents an electrically charged squirk plus neutral squirk system that has settled into its ground state before the $u_\pm$ has had a chance to β-decay. The dominant annihilation channel is $\eta_{\pm 0} \to W^\pm \gamma$, with rate [9]

$$\Gamma(\eta_{\pm 0} \to W^\pm \gamma) = \frac{\pi \alpha \alpha_W N_c N_{ic} s_\theta^2}{(m_0 + m_\pm)^2} f(m_0, m_\pm, m_W) \, |\psi(0)|^2 \tag{29}$$

where $\alpha_W = \alpha / s_W^2$, and the kinematic function $f(m_0, m_\pm, m_W)$ has been relegated to the Appendix B. Whether the timescale for this rate is slower or faster than β-decay depends on the parameters in the model. Small mass splittings tend to suppress β-decay, whereas small Λ_{ic}, which leads to a larger Bohr radius, tends to suppress the annihilation rate. There are potentially additional decay channels, including WZ and Wh, but these are much more suppressed by phase space, and so we will not calculate their widths.

C. η_{+-}

The neutral meson formed from the two charged squirks can also decay into QCD gluons and infracolor gluons, with decay rates identical to Eqs. (27,28) substituting $m_i \to m_\pm$. Since the constituent squirks are electrically charged, η_{+-} can also decay into into photons with a decay rate

$$\Gamma(\eta_{+-} \to \gamma\gamma) = \frac{6\pi N_{ic} \alpha_{\rm em}^2}{m_\pm^2} |\psi(0)|^2 \, . \tag{30}$$

This is an interesting annihilation channel, and potentially a constraint on our model, given existing bounds on $\gamma\gamma$ resonances from collider data. We discuss the size of this signal in the next section.

Finally, there is another uniquely squirky annihilation mode, namely $\eta_{+-} \to u_0 u_0^\dagger$, through the quartic interaction, Eq. (2), proportional to λ_4. The rate for this annihilation is given by

$$\Gamma(\eta_{+-} \to u_0 u_0^\dagger) = \frac{9\pi N_{ic}^2 (\alpha_4 s_\theta^2 + \alpha_{U4} c_\theta^2)^2)}{2 m_\pm^2} \sqrt{1 - \frac{m_0^2}{m_\pm^2}} |\psi(0)|^2 \, . \tag{31}$$

where $\alpha_{4,U4} \equiv \lambda_{4,U4}/(4\pi)$. This so-called "double wonga-wonga" process is unique in that the annihilation is from heavy squirks to light squirks without any hard SM emission. In practice, the light squirks will subsequently spin-down, analogous to the spin-down phase following ordinary collider production of squirks, and then the light squirks bind up into an η_{00} and annihilate as discussed in Sec. V A.

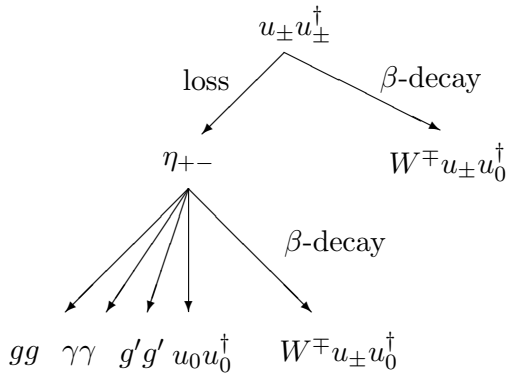

FIG. 6. The "tree of life" for the charged squirk pair. Charged squirk pair tree of life. Everywhere $u_\pm u_0^\dagger$ is written is understood to mean $u_\pm u_0^\dagger + u_0 u_\mp^\dagger$.

VI. BRANCHING FRACTIONS AND SIGNAL ESTIMATES

With the various decay rates in hand we can now compute the total cross sections for several final states of interest. We will again separate the discussion according to the different initial states.

A. $u_\pm u_0^\dagger + u_0 u_\mp^\dagger$

The detailed branching fraction "tree of life" of the quirk pair $u_\pm u_0^\dagger + u_0 u_\mp^\dagger$ is shown in Fig. 5. The first branch splits between β-decay of $u_\pm$ (right branch) versus radiative energy loss, leading to the ground state meson $\eta_{\pm 0}$ (left branch). The relative probabilities of these two branches are set by Eqs. (19) and (20).

Following the left branch, in which the ground state $\eta_{\pm 0}$ is reached, the tree of life then branches further, as the meson $\eta_{\pm 0}$ can decay into several different channels. Considering all possible β-decay branchings of $u_\pm u_0^\dagger$ into $W^\pm u_0 u_0^\dagger$, the relevant branching fraction here is

$$\mathrm{BR}(\eta_{\pm 0} \to W^\pm u_0 u_0^\dagger) = \frac{\Gamma_\beta}{\Gamma_\beta + \Gamma_{W\gamma}} \tag{32}$$

where the Γ_β is given by Eq. (15) and $\Gamma(W\gamma)$ is given by Eq. (29).

Assuming one of the β-decay branches is taken, the tree of life results in the squirk pair $u_0 u_0^\dagger$, which after energy loss, ends in the ground state η_{00}. The branching fraction of η_{00} into visible SM particles is given by

$$\mathrm{BR}(\eta_{00} \to gg) = \frac{\Gamma(\eta_{00} \to gg)}{\Gamma(\eta_{00} \to gg) + \Gamma(\eta_{00} \to g'g')}\,, \tag{33}$$

where the decay rates are given in Sec. V B.

Combining these branching fractions, we obtain the cross section of $u_\pm u_0^\dagger + u_0 u_\mp^\dagger$ into the Wjj final state,

$$\sigma_{\pm 0}(Wjj) = \sigma(p\bar{p} \to u_\pm u_0^\dagger) \left[\mathrm{BR}(u_\pm u_0^\dagger \to W^\pm u_0 u_0^\dagger) + \mathrm{BR}(u_\pm u_0^\dagger \to \eta_{\pm 0})\mathrm{BR}(\eta_{\pm 0} \to W^\pm u_0 u_0^\dagger)\right] \mathrm{BR}(\eta_{00} \to gg) \tag{34}$$

where the two terms in the square bracket represent the two paths to our final state, determined whether β-decay or energy loss occurred first. The cross section into the $W\gamma$ final state is

$$\sigma_{\pm 0}(W\gamma) = \sigma(p\bar{p} \to u_\pm u_0^\dagger) \left[\mathrm{BR}(u_\pm u_0^\dagger \to \eta_{\pm 0})\mathrm{BR}(\eta_{\pm 0} \to W^\pm \gamma)\right]\,. \tag{35}$$

This final state has a bound of about $\sigma_{W\gamma} \lesssim$ 8-13 pb to 95% CL, using constraints from D0 [36] and CDF [37]. The cross sections given for $\sigma(p\bar{p} \to u_\pm u_0^\dagger)$ are understood to sum both $u_\pm u_0^\dagger$ and $u_0 u_\mp^\dagger$ contributions.

B. $u_\pm u_\pm^\dagger$

The tree of life for the $u_\pm u_\pm^\dagger$ is somewhat more complicated and is the result of combining Figs. 6,5. The branching begins between energy loss and β-decay (which is now twice as fast to account for the decay of either squirk) at the top of Fig. 6. If energy loss is fast, the system will typically get to the ground state meson η_{+-} (left branch). Here there are several interesting decay modes, including gg, $g'g'$ (invisible), $\gamma\gamma$,[6] and $u_0 u_0^\dagger$. The latter can play an important role in cases where there is tension with the $\gamma\gamma$ or pre-tagged top constraints. In particular, if $\lambda_4 \sim 2$, the mode Eq. (31) can dominate, effectively diminishing the branching fraction into dangerous modes. We note however that diphoton and pre-tagged top are safe in large regions of our parameter space even in the absence of the λ_4 coupling.

The branching fraction of η_{+-} to β-decay is

$$\mathrm{BR}(\eta_{+-} \to W^\mp u_\pm u_0^\dagger) = \frac{2\Gamma_\beta}{2\Gamma_\beta + \Gamma_{gg} + \Gamma_{g'g'} + \Gamma_{u_0 u_0^\dagger} + \Gamma_{\gamma\gamma}}\,, \tag{36}$$

where $u_\pm u_0^\dagger$ is understood to mean both $u_\pm u_0^\dagger$ and $u_0 u_\mp^\dagger$.

We pay close attention to the $WWjj$ final state, which is the result of the β-decay of both squirks and the subsequent annihilation of η_{00} into dijets. Combining branching fractions, we obtain the cross section for the "two-armed lobster" shown in Fig. 1 into the $WWjj$ final state,

$$\begin{aligned}\sigma_{+-}(WWjj) = \sigma(p\bar{p} \to u_\pm u_\pm^\dagger) \Big[\mathrm{BR}(u_\pm u_\pm^\dagger \to W^\mp u_\pm u_0^\dagger) + \mathrm{BR}(u_\pm u_\pm^\dagger \to \eta_{+-})\mathrm{BR}(\eta_{+-} \to W^\mp u_\pm u_0^\dagger)\Big] \\ \times \Big[\mathrm{BR}(u_\pm u_0^\dagger \to W^\pm u_0 u_0^\dagger) + \mathrm{BR}(u_\pm u_0^\dagger \to \eta_{\pm 0})\mathrm{BR}(\eta_{\pm 0} \to W^\pm u_0 u_0^\dagger)\Big]\, \mathrm{BR}(\eta_{00} \to gg)\end{aligned} \tag{37}$$

where the two terms in each square bracket represent the four distinct paths to our final state, determined whether β-decay or energy loss occurred first in either of Fig. 5 or 6. Again, $u_\pm u_0^\dagger$ is understood to mean both $u_\pm u_0^\dagger$ and $u_0 u_\mp^\dagger$ in the branching ratios, as appropriate. The cross sections of $u_\pm u_\pm^\dagger$ directly into various resonance final states are

$$\sigma_{+-}(ij) = \sigma(p\bar{p} \to u_\pm u_\pm^\dagger) \Big[\mathrm{BR}(u_\pm u_\pm^\dagger \to \eta_{+-})\mathrm{BR}(\eta_{+-} \to ij)\Big]\,, \tag{38}$$

where ij can be any of gg, $g'g'$ (invisible), $\gamma\gamma$, and $u_0 u_0^\dagger$.

The $WWjj$ final state is important for two reasons. First, the $WWjj$ signature can "leak" into the Wjj search when the decay products of one W are either lost or do not pass the CDF analysis cuts for their exclusive analysis. In particular, if the mass splitting $m_\pm - m_0$ is not too large the jets from a hadronically decaying W will be softer, and can frequently fall below analysis cuts on jet E_T. The CDF collaboration analysis for Wjj has a jet energy requirement of $E_T > 30$ GeV, suggesting it is much more likely for the jets from a hadronically decaying off-shell W to *not* pass their E_T cuts. This means that charged squirk pair production provides *an additional production source* of the Wjj signal after detector cuts. As the mass splitting is increased, a decreasing fraction of jets from a hadronically decaying W would *fail* their E_T cut, leading to a smaller contribution to the Wjj signal.

Second, consider the dileptonic process, where both W's decay to e or μ. The signature of this process, $l^\pm l^{(\prime)\mp} jj$ plus missing energy, is nearly identical to top quark production and dileptonic decay, $t\bar{t} \to W^+W^-\bar{b}b$, when b-tagging is *not* required of the jets. This was analyzed by CDF, where their measurements of the fully leptonic "pre-tagged" top cross section implies an upper limit on this signature of about 2 pb at 95% CL [38].

This is likely a reasonable limit for on-shell W-pair production in association with 2 jets. However, off-shell W's can lead to suppression of this signal due to the smaller fraction of events with sufficient energy to pass the detector cuts. We make some rough estimates of the efficiencies of both the Wjj and pre-tagged top analysis in the next section.

Another final state which can potentially constrain the parameter space is the decay of the η_{+-} meson into $\gamma\gamma$. Searches for diphoton resonances were performed by CDF [39], D0 [40], and CMS [41] in the context of RS graviton searches. The constraint on the cross section for a diphoton resonance, in the mass window of interest to us, $2m_\pm \simeq$ 240-290 GeV, is of order 10-40 fb.[7]

---

[6] Note that the final states $W^\pm W^\mp$ and ZZ may also be of interest, particularly at LHC, but are not calculated here.

[7] A more precise number is not straightforward to extract because CDF [39] has a diphoton excess at an invariant mass of 200 GeV, leading to a weak bound of 100 fb (as opposed to the expected 30 fb), while D0 [40] did not present an exclusion plot for $\gamma\gamma$ resonance cross section independent of the ee resonance cross section.

	Bench 1	Bench 2	Exp't Bound
N_{ic}	3	4	-
Λ_{ic}	1.6	6.2	-
M_V	120	145	-
M_S	150	250	-
δ	106.5	172	-
λ_4	2	1	-
m_0	80	75	-
$m_\pm$	120	145	$\gtrsim 100$
m_1	175	279	-
s_θ	0.82	0.89	-
$\sigma(u_0 u_0^\dagger)$	33	42	-
$\sigma(u_\pm u_0^\dagger + u_0 u_\mp^\dagger)$	2.5	1.9	-
$\sigma(u_\pm u_\pm^\dagger)$	6.2	3.5	-
$BR(u_0 u_0^\dagger \to gg)$	0.51	0.48	-
$BR(u_0 u_0^\dagger \to g'g')$	0.49	0.52	-
$\sigma_{\rm UA2}(u_0 u_0^\dagger \to gg)$	0.3	0.6	$\lesssim 90$
$\sigma_{\pm 0}(Wjj)$	0.72	0.84	-
$\sigma_{+-}(WWjj)$	2.4	2.4	-
$\sigma(\ell^+\ell^{-(\prime)}jj) \times$ eff	1.6	2.0	$\lesssim 2$
$\sigma(Wjj) \times$ eff	1.3-2.0	1.0-1.5	$\lesssim 1.9$
$WWjj/Wjj_{\rm total}$	$\sim 85\%$	$\sim 69\%$	-
$\sigma_{+-}(\gamma\gamma)$	0.006	0.004	$\lesssim$ 0.01-0.04
$\sigma_{\pm 0}(W\gamma)$	1.1	0.2	$\lesssim$ 8-14
ΔT	0.02	0.01	$-0.05 \to 0.2$
$\sigma_{\rm LHC7}(u_0 u_0^\dagger)$	480	430	-
$\sigma_{\rm LHC7}(u_\pm u_\pm^\dagger)$	200	130	-

TABLE II. Benchmark models in parameter space. All masses in GeV, all cross sections are in pb for Tevatron (except "LHC7" for $\sqrt{s} = 7$ TeV LHC and "UA2" for $\sqrt{s} = 630$ GeV CERN SppS). The cross sections are discussed in Sec. III, the branching fractions into various final states discussed in Sec. VI, the efficiencies are discussed in Sec. VII, and ΔT calculation is done in Sec. A.

VII. BENCHMARKS AND EFFICIENCIES

We present two benchmarks with the parameters, masses, cross sections, branching fractions in Table II. The two benchmarks represent two qualitatively different regimes: Benchmark 1 has rapid spin-down, and then squirky β-decay or annihilation, whereas Benchmark 2 has rapid β-decay, and then annihilation. Each Benchmark results in qualitatively distinct signal kinematics, as we will explain. For each Benchmark, we also present our estimates of the relevant limits on certain parameters and signal rates. The input parameters are $N_{ic}, M_V, M_S, \delta, \lambda_4$. We took $N_{ic} = 3, 4$ infracolors for Benchmark 1,2, leading to a signal rate into dijets that easily satisfies the UA2 bound. We took M_V, M_S, δ such that the masses worked out to $m_\pm, m_0 = 120, 80$ GeV and $m_\pm, m_0 = 145, 75$ GeV. This allows us to illustrate the qualitative differences between $\Delta m = 40$ GeV versus $\Delta m = 70$ GeV. We chose M_S to be slightly heavier than M_V, such that the contributions to the isospin-violating electroweak correction, ΔT, essentially vanish, as described in Appendix A. Finally, we took λ_4 to be of order one, which ensures the cross section $\sigma_{+-}(\gamma\gamma)$ is less than 10 fb. Smaller values of λ_4 imply larger rates, of order tens of fb, into diphotons.

The cross sections $\sigma(u_0 u_0^\dagger)$, $\sigma(u_\pm u_0^\dagger + u_0 u_\mp^\dagger)$, and $\sigma(u_\pm u_\pm^\dagger)$ can be read off from Figs. 2,3. Weak production is suppressed by couplings, while the colored production of $\sigma(u_\pm u_\pm^\dagger)$ is enhanced by couplings but further suppressed by kinematics, leading to rates at the Tevatron that are roughly comparable.

Each model has $\Lambda_{ic} \ll m_{\rm squirk}$, such that the infracolor coupling, $\alpha_{ic}(m_q)$, is perturbative when evaluated at the mass of the squirk. The choice $\Lambda_{ic} \sim$ few GeV implies infraglueballs decay well outside the detector, but decay fast enough to not cause cosmological conundrums. Hence, the $g'g'$ final state leads to no hard SM particles, and possibly missing energy (depending on the decay kinematics).

The cross sections $\sigma_{\pm 0}(Wjj)$ and $\sigma_{+-}(WWjj)$ correspond to Eqs. (34) and (37) respectively. These cross sections form the starting point for obtaining the Wjj signal, as well as several additional signals for which the Tevatron has already placed constraints.

We have then estimated the efficiency to detection for three signals: the efficiency for $\sigma_{\pm 0}(Wjj)$ to pass the CDF Wjj analysis cuts [1], the efficiency for $\sigma_{+-}(WWjj)$ to pass the CDF Wjj analysis cuts (where one W's decay

products are missed or not energetic enough to pass the CDF cuts), and finally, the efficiency for $\sigma_{+-}(WWjj)$ to pass the CDF $t\bar{t}$ pre-tag analysis cuts [38], which we call $\sigma(\ell^+\ell^{-(\prime)}jj) \times$ eff.

Our estimates are based on a "stand-in" model for squirk production and decay, modeled as intermediate resonances with masses the same as η_{+-}, $\eta_{\pm 0}$ and η_{00}, allowing for β-decay into $\eta_{\pm 0}$ which in turn can β-decay into η_{00}. We have implemented both of these models in MadGraph [42] with various mass splittings. The modeling of missing energy cannot be reliably done, given the squirky spin-down process that can emit infraglueballs which escape the detector as missing energy.

Nevertheless, we can implement the various lepton, jet, missing energy and transverse mass cuts on the "stand in" model to obtain "stand in" efficiencies which should give us a reasonable idea of where the squirk model stands with respect to the various signals after cuts. Both benchmarks lead to some excess in the dileptonic pre-tag $t\bar{t}$ sample ($\sigma(\ell^+\ell^{-(\prime)}jj)$ plus missing energy), but within the 95% CL limit from CDF. Both benchmarks also lead to between 1-2 pb of Wjj signal, where the range corresponds to including (not including) the missing energy and transverse mass cuts for the lower (upper) end of the range shown. Also shown in Table II is the ratio $WWjj/Wjj_{\rm total}$ which corresponds to the fraction of Wjj signal after efficiencies that arise from the two-armed lobster versus the one-armed lobster. We conclude that the squirk model we have presented is capable of generating a Wjj signal consistent with the CDF excess, so long as the efficiency of detection of squirks is comparable to our "stand in" model for event-level simulation.

While we have presented estimates for a variety of observables above, we emphasize that several quantities should be taken as rough estimates due to the various uncertainties involving quirky dynamics. For example, the uncertainty on the timescale of energy loss can strongly affect the branching fractions between spin-down and β-decay as shown in Fig. 5 and 6. In addition, squirks that rapidly lose energy often reach the η ground states, which have definite masses, and so leads to features in kinematic distributions. Even when energy loss is rapid, the choice between branchings involving β-decay (such as Wjj and $WWjj$) versus annihilation channels (such as $W\gamma$ and $\gamma\gamma$) is sensitive to the uncertainty in the wavefunction at the origin for quirkonium states.

VIII. IMPLICATIONS AND DISCUSSION

We have demonstrated that the Wjj signal observed by CDF can be obtained from a model of squirks without violating existing collider bounds. There are two qualitative regimes where the signal arises:

1. Rapid spin-down, then squirky β-decay or annihilation. In this scenario, the excess energy squirks carry, $\sqrt{\hat{s}}-2m$, is released quickly, allowing the squirk pair production to settle into squirkonium. This could happen because β-decay is suppressed, or could happen if the energy loss is rapid, or both.

   A competition is set up between β-decay of the squirkonium constituent squirks versus direct annihilation of the squirks. In this regime, several interesting squirkonium decay modes with invariant mass resonances are potential confirmation signals, including gg, $W\gamma$, $\gamma\gamma$, $g'g'$ (invisible), and possibly $W^\pm W^\mp$, $W^\pm Z$, ZZ, and signals with a Higgs boson.

2. Rapid β-decay, then spin-down, then annihilation. In this regime, the only squirkonium state that is reached is η_{00}, yielding the famous jet-jet resonance. This could happen if β-decay is comparatively fast, or could happen if energy loss is comparatively slow, or both.

   In this regime, every heavy squirk β-decay yields a (possibly off-shell) W, giving many signals with multi-W's plus a jet-jet resonance.

The two regimes share several interesting signals including the Wjj final state. Interestingly, neither regime contains an associated γjj or Zjj signal, which is characteristic of this model. We emphasize that while squirk production and squirk β-decay rates can be calculated perturbatively, the "spin-down" or energy loss phase, as well as the squirkonium decay rates have substantial uncertainties. The relative branching fractions of squirkonium can in some cases be determined, since the decay rate dependence on the wave function at the origin drops out. But determining which of energy loss or β-decay is more rapid can merely be estimated.

The kinematics of the two regimes to Wjj are qualitatively distinct. In particular, if the second term dominates one would expect an invariant mass peak for the whole Wjj system, and an edge in the transverse mass distribution, while if the second dominates such features would be either absent, or less pronounced. CDF have presented interesting distributions [2], but we leave the investigation of such kinematic features for future work.

We have calculated the LHC production cross sections of the squirks in the parameter ranges relevant to this model. We find that the electroweak production of charged plus neutral squirks is relatively small, typically a few pb. The colored production of squirks is, not surprising, quite large – of order hundreds of pb! The LHC production of $u_\pm u_\pm^\dagger$

seems particularly important, since depending on which regime we are in, it can yield signal rates into the annihilation modes [regime 1] or the multi-W production [regime 2].

There are several associated signals of our model that we have not discussed. Squirks have nontrivial interactions with the Higgs boson through the dimension-4 operator, Eq. (3). Loops of squirks modify the effective hgg coupling as well as $h\gamma\gamma$. Since u_0, u_1 receives its mass from both electroweak preserving, Eq. (1) and electroweak breaking Eq. (3), the contribution will scale as $\delta^2/(\delta^2 + M^2)$.

In this paper we have focused mainly on a quirky explanation for the CDF Wjj excess, but in the process we have illustrated many interesting signals of quirk or squirk production at colliders. With the Tevatron hints of new physics, combined with the wonderful prospects at LHC, we expect an exciting time in quirky physics.

Note added: Just before this paper was completed, D0 reported an analysis of their Wjj data, finding "no evidence for anomalous resonant dijet production" [43]. Taken at face value, their analysis sets an upper bound of 1.9 pb at 95% CL for resonant dijet production near the invariant mass window of the CDF excess, and thus does not rule out a new physics explanation of the CDF excess with a cross section less than this value. Given that the D0 analysis was done with lower luminosity (4.3 fb^{-1} [43] versus 7.3 fb^{-1} [2]), without an inclusive (2 or more jets) analysis (unlike [2]), we remain skeptical of drawing negative conclusions until the joint task force [44] completes their analysis.

Appendix A: Electroweak Precision Corrections

The introduction of the Higgs operator at dimension-4, Eq. (3), splits the masses of the fields within the triplet V. This isospin violation leads to modifications to electroweak precision data. The correction to S, which characterizes $B_\mu \leftrightarrow W^0_\mu$ mixing induced by electroweak symmetry breaking, vanishes here since the squirks transform in electroweak representations with zero hypercharge.

The correction to T arises from the mass difference between the charged and neutral components of the isotriplets. This has been calculated for a general scalar multiplet with arbitrary isospin and hypercharge in Ref. [45]. Applying their results to our case, we obtain

$$\Delta T = \frac{N_c N_{ic}}{16\pi s_w^2 M_W^2}\left[c_\theta^2 f(m_0, m_\pm) - s_\theta^2 f(m_1, m_\pm)\right] \tag{A1}$$

in terms of the self-energy loop function

$$f(m_a, m_b) = m_a^2 + m_b^2 - \frac{2m_a^2 m_b^2}{m_a^2 - m_b^2}\log\frac{m_a^2}{m_b^2} \tag{A2}$$

As expected for a renormalizable theory, the correction to T is finite, and vanishes in the various limits: $m_0 \to m_1$ (the operator vanishes); $m_V \gg m_S$ (decouple the V scalar); and $m_S \gg m_V$ (decouple the S scalar).

Since the model contains negligible additional contributions to ΔS, the quantity ΔT can be bounded from fits to S and T, e.g. [46], where one can allow $-0.05 \lesssim \Delta T \lesssim 0.2$ and remain within the 95% CL limits for $m_h = 115$ GeV. Wide ranges of parameters allow for sizeable splitting between the charged and neutral squirks (allowing weak decay to proceed, c.f. Sec.IV A), while having T easily within the electroweak bounds.

Appendix B: Collected Formulae

Here we collect some analytic formulae used in earlier parts of the paper. The function f used in Eq. (35) for the weak annihilation of $\eta_{\pm 0}$ into $W\gamma$ is

$$f(m_0, m_\pm, m_W) = \frac{\left[(m_0+m_\pm)^2 - m_W^2\right]\left[m_W^2\left(-3m_0^2 + 4m_0 m_\pm + 3m_\pm^2\right) + m_0(m_0^2 - m_\pm^2)(3m_0 + m_\pm)\right]}{2m_0 m_\pm^2 m_W^2 (m_0 + m_\pm)} \tag{B1}$$

The function R used in the formula for the beta decay rate of $u_\pm \to u_0 + W^*$ in Eq. (15) is

$$\begin{aligned} R(m_\pm, m_0, m_W) = {} & \frac{9m_W^4\left(m_\pm^4 - m_0^4\right) + 2m_W^2\left(m_0^2 - m_\pm^2\right)^3 + 6m_W^6(m_0^2 - m_\pm^2)}{m_\pm^3} \\ & + 6\frac{m_W^4}{m_\pm^3}\left\{\tilde{\Delta}^2\left(m_0^2 + m_\pm^2 - m_W^2\right)\left[\tan^{-1}\left(\frac{m_0^2 - m_\pm^2 + m_W^2}{\hat{\Delta}^2}\right) - \tan^{-1}\left(\frac{-m_0^2 + m_\pm^2 + m_W^2}{\tilde{\Delta}^2}\right)\right]\right. \\ & \left. - \left[m_0^4 + m_\pm^4 + m_W^4 - 2m_W^2\left(m_0^2 + m_\pm^2\right)\right]\log\left(\frac{m_0}{m_\pm}\right)\right\} \end{aligned} \tag{B2}$$

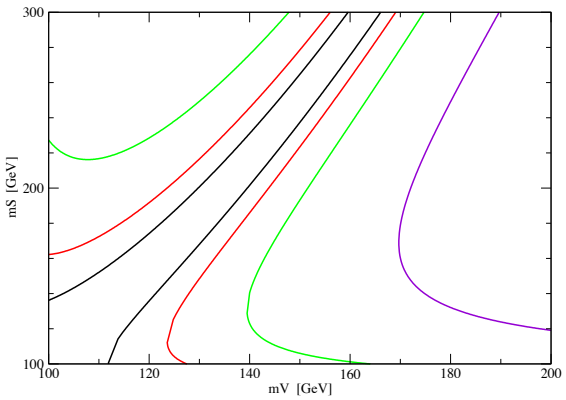

FIG. 7. Contours of ΔT *per infracolor*, but including QCD color, in the (m_U, m_S) parameter space. From left to right the contours are $-0.1, -0.05, -0.025, +0.025, 0.05, 0.1, 0.25$. The "funnel" region has $\Delta T \simeq 0$ due to a cancellation between the loops of the light and heavy neutral scalars.

where

$$\tilde{\Delta}^2 \equiv \sqrt{(m_0 + m_\pm - m_W)(m_0 - m_\pm + m_W)(-m_0 + m_\pm + m_W)(m_0 + m_\pm + m_W)} \tag{B3}$$

and

$$\hat{\Delta}^2 \equiv \sqrt{(-m_0 + m_\pm + m_W)(m_0 + m_\pm - m_W)(m_0 - m_\pm + m_W)(m_0 + m_\pm + m_W)} \tag{B4}$$

ACKNOWLEDGMENTS

We thank Z. Chacko, R. Fok and M. Strassler for useful conversations. GDK was supported by a Ben Lee Fellowship from Fermilab and in part by the US Department of Energy under contract number DE-FG02-96ER40969. RH, GDK, AM are supported by Fermilab operated by Fermi Research Alliance, LLC under contract number DE-AC02-07CH11359 with the US Department of Energy.

[1] T. Aaltonen *et al.* [CDF Collaboration], arXiv:1104.0699 [hep-ex].
[2] A. Annovi, P. Catastini, V. Cavaliere, and L. Ristori, `http://www-cdf.fnal.gov/physics/ewk/2011/wjj/7_3.html`.
[3] E. J. Eichten, K. Lane and A. Martin, arXiv:1104.0976 [hep-ph].
[4] M. R. Buckley, D. Hooper, J. Kopp, E. Neil, [arXiv:1103.6035 [hep-ph]]; F. Yu, arXiv:1104.0243 [hep-ph]; C. Kilic and S. Thomas, arXiv:1104.1002 [hep-ph]; K. Cheung and J. Song, arXiv:1104.1375 [hep-ph]; J. A. Aguilar-Saavedra and M. Perez-Victoria, arXiv:1104.1385 [hep-ph]; X. G. He and B. Q. Ma, arXiv:1104.1894 [hep-ph]; X. P. Wang, Y. K. Wang, B. Xiao, J. Xu and S. h. Zhu, arXiv:1104.1917 [hep-ph]; R. Sato, S. Shirai and K. Yonekura, arXiv:1104.2014 [hep-ph]; A. E. Nelson, T. Okui and T. S. Roy, arXiv:1104.2030 [hep-ph]; L. A. Anchordoqui, H. Goldberg, X. Huang, D. Lust and T. R. Taylor, arXiv:1104.2302 [hep-ph]; B. A. Dobrescu and G. Z. Krnjaic, arXiv:1104.2893 [hep-ph]; G. Zhu, arXiv:1104.3227 [hep-ph]; P. Ko, Y. Omura and C. Yu, arXiv:1104.4066 [hep-ph]; T. Plehn and M. Takeuchi, arXiv:1104.4087 [hep-ph]; P. J. Fox, J. Liu, D. Tucker-Smith and N. Weiner, arXiv:1104.4127 [hep-ph]; D. W. Jung, P. Ko and J. S. Lee, arXiv:1104.4443 [hep-ph]; S. Chang, K. Y. Lee and J. Song, arXiv:1104.4560 [hep-ph]; H. B. Nielsen, arXiv:1104.4642 [hep-ph]; B. Bhattacherjee and S. Raychaudhuri, arXiv:1104.4749 [hep-ph]; Q. H. Cao, M. Carena, S. Gori, A. Menon, P. Schwaller, C. E. M. Wagner and L. T. M. Wang, arXiv:1104.4776 [hep-ph]; K. S. Babu, M. Frank and S. K. Rai, arXiv:1104.4782 [hep-ph]; B. Dutta, S. Khalil, Y. Mimura and Q. Shafi, arXiv:1104.5209 [hep-ph]; X. Huang, [arXiv:1104.5389 [hep-ph]]; J. E. Kim, S. Shin, [arXiv:1104.5500 [hep-ph]]; L. M. Carpenter, S. Mantry, [arXiv:1104.5528 [hep-ph]]; G. Segre, B. Kayser, [arXiv:1105.1808 [hep-ph]]; T. Enkhbat, X. -G. He, Y. Mimura, H. Yokoya, [arXiv:1105.2699 [hep-ph]]; C. -H. Chen, C. -W. Chiang, T. Nomura, Y. Fusheng, [arXiv:1105.2870 [hep-ph]]; D. Bettoni, P. Dalpiaz, P. F. Dalpiaz, M. Fiorini, I. Masina and G. Stancari, arXiv:1105.3661 [hep-ex]; Z. Liu, P. Nath and G. Peim, arXiv:1105.4371 [hep-ph]; A. Hektor, G. Hutsi, M. Kadastik, K. Kannike, M. Raidal and D. M. Straub, arXiv:1105.5644 [hep-ph];

J. L. Hewett and T. G. Rizzo, arXiv:1106.0294 [hep-ph]; J. Fan, D. Krohn, P. Langacker and I. Yavin, arXiv:1106.1682 [hep-ph].
[5] J. M. Campbell, A. Martin and C. Williams, arXiv:1105.4594 [hep-ph].
[6] L. B. Okun, JETP Lett. **31**, 144 (1980) [Pisma Zh. Eksp. Teor. Fiz. **31**, 156 (1979)]; L. B. Okun, Nucl. Phys. B **173**, 1 (1980); J. D. Bjorken, (1979), SLAC-PUB-2372; S. Gupta and H. R. Quinn, Phys. Rev. D **25**, 838 (1982).
[7] J. Kang and M. A. Luty, JHEP **0911**, 065 (2009) [arXiv:0805.4642 [hep-ph]].
[8] G. Burdman, Z. Chacko, H. S. Goh and R. Harnik, JHEP **0702**, 009 (2007) [arXiv:hep-ph/0609152].
[9] G. Burdman, Z. Chacko, H. S. Goh, R. Harnik and C. A. Krenke, Phys. Rev. D **78**, 075028 (2008) [arXiv:0805.4667 [hep-ph]].
[10] K. Cheung, W. Y. Keung and T. C. Yuan, Nucl. Phys. B **811**, 274 (2009) [arXiv:0810.1524 [hep-ph]].
[11] R. Harnik and T. Wizansky, Phys. Rev. D **80**, 075015 (2009) [arXiv:0810.3948 [hep-ph]].
[12] H. Cai, H. C. Cheng and J. Terning, JHEP **0905**, 045 (2009) [arXiv:0812.0843 [hep-ph]].
[13] C. Kilic, T. Okui and R. Sundrum, JHEP **1002**, 018 (2010) [arXiv:0906.0577 [hep-ph]].
[14] S. Chang and M. A. Luty, arXiv:0906.5013 [hep-ph].
[15] S. Nussinov, C. Jacoby, [arXiv:0907.4932 [hep-ph]].
[16] G. D. Kribs, T. S. Roy, J. Terning and K. M. Zurek, Phys. Rev. D **81**, 095001 (2010) [arXiv:0909.2034 [hep-ph]].
[17] C. Kilic and T. Okui, JHEP **1004**, 128 (2010) [arXiv:1001.4526 [hep-ph]].
[18] L. Carloni and T. Sjostrand, JHEP **1009**, 105 (2010) [arXiv:1006.2911 [hep-ph]].
[19] S. P. Martin, Phys. Rev. D **83**, 035019 (2011) [arXiv:1012.2072 [hep-ph]].
[20] R. Fok, G.D. Kribs, to appear.
[21] R. Harnik, G. Y. Huang, M. Luty, S. Mrenna, in progress.
[22] M. J. Strassler and K. M. Zurek, Phys. Lett. B **651**, 374 (2007) [arXiv:hep-ph/0604261].
[23] T. Han, Z. Si, K. M. Zurek and M. J. Strassler, JHEP **0807**, 008 (2008) [arXiv:0712.2041 [hep-ph]].
[24] M. J. Strassler, arXiv:0806.2385 [hep-ph].
[25] For example, see K. J. Juge, J. Kuti, C. J. Morningstar, Nucl. Phys. Proc. Suppl. **63**, 326-331 (1998). [hep-lat/9709131].
[26] V. M. Abazov *et al.* [D0 Collaboration], Phys. Rev. Lett. **105**, 211803 (2010) [arXiv:1008.3547 [hep-ex]].
[27] T. Aaltonen *et al.* [CDF Collaboration], Phys. Rev. D **79**, 112002 (2009) [arXiv:0812.4036 [hep-ex]].
[28] J. Alitti *et al.* [UA2 Collaboration], Nucl. Phys. B **400**, 3 (1993).
[29] LEPEWWG $f\bar{f}$ Subgroup, LEP2FF/02-03, `http://lepewwg.web.cern.ch/LEPEWWG/lep2/summer2002/summer2002.ps`.
[30] V. D. Barger, E. W. N. Glover, K. Hikasa, W. Y. Keung, M. G. Olsson, C. J. . Suchyta and X. R. Tata, Phys. Rev. D **35**, 3366 (1987) [Erratum-ibid. D **38**, 1632 (1988)] [Phys. Rev. D **38**, 1632 (1988)].
[31] M. Drees and M. M. Nojiri, Phys. Rev. D **49**, 4595 (1994) [arXiv:hep-ph/9312213].
[32] S. P. Martin, Phys. Rev. D **77**, 075002 (2008) [arXiv:0801.0237 [hep-ph]].
[33] S. P. Martin and J. E. Younkin, Phys. Rev. D **80**, 035026 (2009) [arXiv:0901.4318 [hep-ph]].
[34] M. Beneke, Y. Kiyo, A. A. Penin, Phys. Lett. **B653**, 53-59 (2007). [arXiv:0706.2733 [hep-ph]]; M. Beneke, Y. Kiyo, K. Schuller, Phys. Lett. **B658**, 222-229 (2008). [arXiv:0705.4518 [hep-ph]].
[35] We thank Z. Chacko for emphasizing this point to the more stubborn author.
[36] D0 Collaboration, D0 Note 6172-CONF, `http://www-d0.fnal.gov/Run2Physics/WWW/results/prelim/EW/E36/E36.pdf`.
[37] B. Heinemann and A. Nagano [CDF Collaboration], `http://www-cdf.fnal.gov/physics/ewk/2007/wgzg/`
[38] CDF Collaboration, Conf. Note 10163, `http://www-cdf.fnal.gov/physics/new/top/2010/xsection/ttbar_dil_xsec_5invfb/cdfpubnote.pdf`.
[39] T. Aaltonen *et al.* [CDF Collaboration], Phys. Rev. D **83**, 011102 (2011) [arXiv:1012.2795 [hep-ex]].
[40] V. M. Abazov *et al.* [The D0 Collaboration], Phys. Rev. Lett. **104**, 241802 (2010) [arXiv:1004.1826 [hep-ex]].
[41] S. Chatrchyan *et al.* [CMS Collaboration], JHEP **1105**, 085 (2011) [arXiv:1103.4279 [hep-ex]].
[42] J. Alwall, P. Demin, S. de Visscher, R. Frederix, M. Herquet, F. Maltoni, T. Plehn, D. L. Rainwater *et al.*, JHEP **0709**, 028 (2007). [arXiv:0706.2334 [hep-ph]].
[43] D0 Collaboration, arXiv:1106.1921 [hep-ex].
[44] CDF, D0, E. Eichten, and K. Ellis, `http://www.fnal.gov/pub/today/archive_2011/today11-06-10_readmore.html`.
[45] L. Lavoura and L. F. Li, Phys. Rev. D **49**, 1409 (1994) [arXiv:hep-ph/9309262].
[46] G. D. Kribs, T. Plehn, M. Spannowsky and T. M. P. Tait, Phys. Rev. D **76**, 075016 (2007) [arXiv:0706.3718 [hep-ph]].